

Bioactive sol–gel glass added ionomer cement for the regeneration of tooth structure

Jung-Young Choi · Hae-Hyoung Lee ·
Hae-Won Kim

Received: 15 October 2007 / Accepted: 25 April 2008 / Published online: 16 May 2008
© Springer Science+Business Media, LLC 2008

Abstract Dental cements including the glass ionomer cement (GIC) have found widespread use in restoring tooth structures. In this study, a sol–gel derived glass (SG) with a bioactive composition ($70\text{SiO}_2 \cdot 25\text{CaO} \cdot 5\text{P}_2\text{O}_5$) was added to the commercial GIC (GC, Fuji I) to improve the bioactivity and tooth regeneration capability. The SG powders prepared with sizes in the range of a few micrometers were mixed with GIC at SG/GC ratios of 10 and 30 wt%. The setting time, diametral tensile strength, and in vitro bioactivity of the GC–SG cements were examined. The setting time of the GC–SG cements increased with increasing amount of SG. However, the addition of SG did not significantly alter the diametral tensile strength of the GC. GC–SG induced the precipitation of an apatite bone-mineral phase on the surface after immersion in a simulated body fluid (SBF), showing in vitro bone bioactivity. However, no mineral induction in SBF was observed in the commercial GIC after the immersion. The in vitro cell assay confirmed that the GC–SG samples produced higher cell viability than the GC sample with cell culturing for up to 7 days.

1 Introduction

Glass ionomer cements (GICs), which were originally developed for use as restorative dental materials more than three decades ago, have found widespread applications in dentistry [1, 2]. Their utility is mainly due to the direct bonding to the tooth structure and the release of fluoride ions that protect against dental caries [3–7]. Compared with the other restorative materials, GICs are relatively biocompatible in the mouth, with no significant harmful biological reactions being reported thus far [8, 9].

Together with their popular use as a luting agent and direct filling restorative in dentistry, GICs are attracting increasing interest for the regeneration of hard tissues including the bone and tooth structure [10–12]. Over the past decades, GICs have also been developed as bone cements in orthopedics, overcoming some of the weaknesses of acrylic-based bone cements (polymethyl methacrylate: PMMA) [13, 14]. The main advantages of GICs over PMMA include good adhesion to the bone, minimal polymerization shrinkage and no significant heat evolution during setting [13, 14]. The self-setting capacity of GICs in a body fluid is considered to be potentially applicable in the bone reconstruction area.

Practically, the currently available GICs have some drawbacks for use in regenerative applications, which mainly include the weakness of the mechanical properties, such as strength and toughness, as well as their poor osteogenic potential to regulate the bone cell functions [15–18]. Although significant consideration has been raised as to the aluminum-associated effect on the brain diseases [13, 19], and it is thus required to develop some new compositions, more studies on the improvement of those aspects should be carried out to find future applications of GICs in the regeneration area.

J.-Y. Choi · H.-H. Lee · H.-W. Kim (✉)
Department of Biomaterials Science, School of Dentistry,
Dankook University, Cheonan 330-714, South Korea
e-mail: kimhw@dku.edu

H.-H. Lee · H.-W. Kim
Institute of Tissue Regeneration Engineering (ITREN),
Dankook University, Cheonan 330-714, South Korea

J.-Y. Choi
Department of Dental Hygiene, Shinsung University,
Choong-Nam 343-861, South Korea

Recent studies reported the modification of commercial GICs with bioactive compositions, such as 45S5 bioglass and hydroxyapatite (HA) powders to improve the biocompatibility of the cements [20, 21]. Moreover, strong powders such as metals (stainless steel) and bioinert ceramics (zirconia) have been incorporated to improve the mechanical properties of the GICs [22, 23]. The results have indicated that secondary powders have some value in the small replacement of GIC powders. Although GICs have attracted considerable interest for use in the hard tissue regenerative areas, studies on bioactive-GICs are still in the early stages.

The aim of this study was to produce a bioactive cement composition by combining the commercially available GIC with bioactive glass powders derived from a sol–gel process. The setting time, mechanical properties and in vitro bioactivity of the developed cements were examined.

2 Materials and methods

2.1 Fabrication of bioactive GICs

For the preparation of experimental sol–gel glass powders, firstly, the glass precursors (tetraethyl orthosilicate, calcium nitrate and triethyl phosphate) were homogenized in sequence within ethanol/water containing 2% HCl (1 N), and then followed by aging and heat treatment at 700°C to prepare the glass granules with a composition of $70\text{SiO}_2 \cdot 25\text{CaO} \cdot 5\text{P}_2\text{O}_5$. The obtained glass granules were crushed and pulverized to a fine powder with zirconia balls (designated as ‘SG’). X-ray diffraction confirmed the phase of the powder to be glass showing no characteristic crystalline peaks. The bioactive glass powder was mixed homogeneously with the commercially available GIC (GC Fuji I, GC Corp., Tokyo, Japan) at two different SG/GC ratios, 10 and 30 wt%, by a ball-milling with zirconia balls. The final cement compositions were GC, GC plus 10 wt% SG and GC plus 30 wt% SG, which are designated as GG, GC–10SG, and GC–30SG, respectively.

2.2 Characterization and mechanical test

The morphology of the powders and hardened samples were characterized by scanning electron spectroscopy (SEM, Hitachi). Transmission electron microscopy (TEM, CM20) was conducted to analyze the nanostructure of the samples. The setting time of the cements was measured in accordance with ISO1566 on the samples prepared at different compositions and powder/liquid ratios. Three replicate samples for each condition were tested.

The mechanical properties of the prepared cements were observed on the samples without and with the incubation in

SBF for 1, 3 and 10 days. Instron 4330 was used to test the diametral tensile strength (DTS) of the cement specimens prepared in a cylindrical type (10 mm × 5 mm) with a 100 kN load cell and a crosshead speed of 1.0 mm/min. The maximum applied loads recorded upon fracture were converted to a DTS value using the following equation: $\text{DTS} = 2P/\pi DL$, where P is the maximum applied load (N), D is the diameter of the sample and L is the length of the sample. A total of 10 specimens were tested for each condition.

2.3 Surface bioactivity

The surface bioactivity of the cements was assessed by immersion in a simulated body fluid (SBF), which has a similar ionic concentration to human body plasma (refer to Table 1). The specimens were prepared in a disc type with dimensions of $\phi 10 \text{ mm} \times 2 \text{ mm}$, kept at room temperature for 24 h and then immersed in SBF at 37°C for various time points. After immersion, the samples were removed, washed with distilled water/ethanol, and examined by SEM to determine the changes in the surface morphology. The change in weight of the samples during incubation was measured using an electronic balance.

2.4 Cell adhesion and viability

Murine-derived osteoblastic cells (MC3T3-E1) were used to assess the cell viability on the cement samples. The cells were maintained in a regular medium [α -modified minimum essential medium (α -MEM) and 1% antibiotic/antimycotic supplemented with 10% fetal bovine serum (FBS)] in a humidified atmosphere containing 5% CO₂/95% air at 37°C. Three different cements (GC, GC–10SG, GC–30SG) were prepared with dimensions of $\phi 10 \text{ mm} \times 5 \text{ mm}$. The samples were placed in each well of a 24 well-plate, washed twice with PBS and dried before the cell test. The cells were seeded on each sample at a density of 3×10^4 cells/specimen and cultured for up to 7 days. At each culturing period (1, 3 and 7 days), the cells were harvested and the cell viability was measured as the mitochondrial NADH/NADPH-dependant dehydrogenase

Table 1 Ionic concentrations of the prepared SBF and human body plasma

	Ionic concentration (mM)							
	Na ⁺	K ⁺	Mg ²⁺	Ca ²⁺	Cl ⁻	HCO ₃ ⁻	HPO ₄ ²⁻	SO ₄ ²⁻
SBF	142.0	5.0	1.5	2.5	147.8	4.2	1.0	0.5
Human body plasma	142.0	5.0	1.5	2.5	103.3	27.0	1.0	0.5

activity using a cell proliferation assay kit (CellTiter 96 Aqueous One Solution, Promega). A colorimetric measurement was performed using a Microplate Reader at an absorbance of 490 nm. Five specimens for each condition were tested ($n = 5$). The cell growth morphology was observed by SEM at an accelerating voltage of 15 kV after fixing with glutaraldehyde (2.5%), dehydrating with a graded series of ethanol (75%, 90%, 95% and 100%), treating with hexamethyldisilazane and Pt-coating.

2.5 Statistics

Data were expressed as mean \pm one standard deviation (SD). Statistical analysis was performed using ANOVA followed by a Bonferroni correction. A P value <0.05 and 0.01 was considered significant.

3 Results and discussion

3.1 Powder characteristics

The nanostructure of the sol–gel derived glass powder, as examined by TEM, is shown in Fig. 1a. The image shows a highly mesoporous structure with pore sizes ranging from a few to tens of nanometers. When the sol–gel glass was immersed in the SBF for 5 days, precipitates of apatite bone-mineral were observed throughout the surface of the glass granules, as shown in Fig. 1b, c, confirming good

bone bioactivity of the sol–gel glass with the composition prepared herein. In practice, the SBF-immersion test is commonly used to predict the bone-forming ability of a biomaterial through an examination of the in vitro formation of bone-mineral apatite upon the material surface. It is believed that such a high bioactivity of the sol–gel glass is mainly due to the highly mesoporous structure of the glass, which is somewhat different from the case in the melt-derived glass [24, 25]. The sol–gel obtained bioactive glass powder was further mixed with the ionomer cement powder to produce 10 and 30 wt% sol–gel glass added cement powders.

Figure 2 shows the characteristic morphology of the sol–gel glass powder (a), the ionomer cement glass powder (b), and their mixture powders (c, d). Although the initial sol–gel glass was in the form of large granules, it was possible to reduce the particle size by a ball-milling. The sol–gel glass and ionomer glass powders had a similar size and morphology. Most were fine powders (less than a few micrometers) but there were also some large-sized powders ($\sim 10 \mu\text{m}$) to be observed. The average sizes of the powders were 3.21 and 2.45 μm for the sol–gel glass and ionomer cement glass, respectively, and 2.58 and 2.73 μm for the 10% and 30% sol–gel glass added powders.

3.2 Properties of cements

The setting time of the cements was measured using a Vicat needle test. Cements with three different

Fig. 1 (a) TEM image of the mesoporous structured sol–gel glass and (b, c) SEM surface morphology of the sol–gel glass powders before (b) and after (c) immersion in the SBF for 5 days. A number of bone-mineral apatite nanocrystallines were precipitated on the surface of the glass granules, confirming the excellent in vitro bone bioactivity

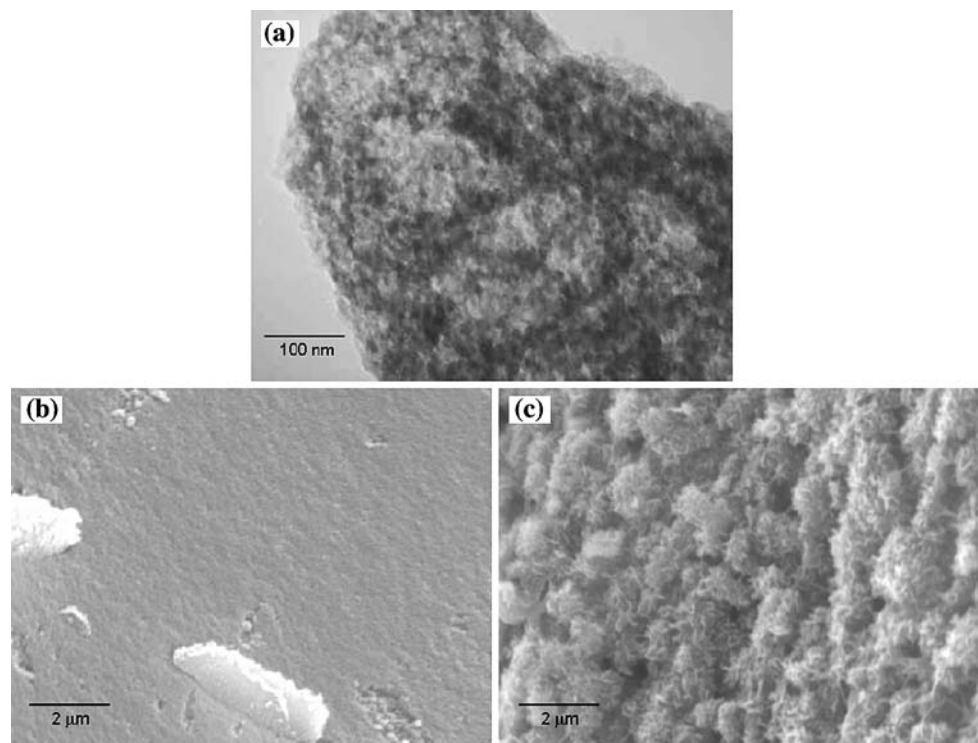
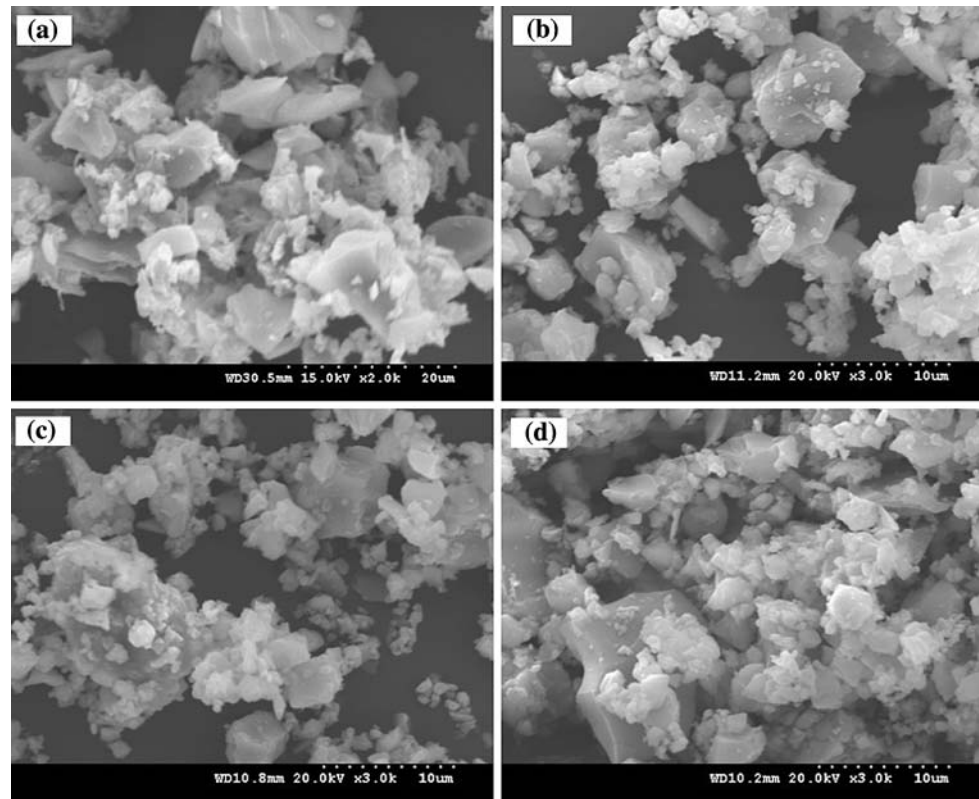


Fig. 2 SEM morphology of the initial and mixture powders used for preparing the dental cements: (a) sol-gel glass, (b) ionomer cement glass, (c) 10% sol-gel glass + ionomer cement glass, and (d) 30% sol-gel + ionomer cement glass



compositions prepared by varying the ratio of powder to liquid (P/L) were tested. As shown in Fig. 3, the setting time decreased with increasing P/L for all compositions. However, the setting time increased with increasing amount of the sol-gel glass. The added sol-gel glass was considered to hinder the hardening process of the ionomer cement, which is mainly driven by the cationic release

from the aluminofluorosilicate glass granules associated with the acid-base reaction [26]. On the other hand, in the sol-gel glass, of which the composition was specifically designed for bone bioactivity, such a cationic release was not considered to proceed significantly. However, although the sol-gel glass powder was observed to retard the setting reaction of the cement, the range of the setting times

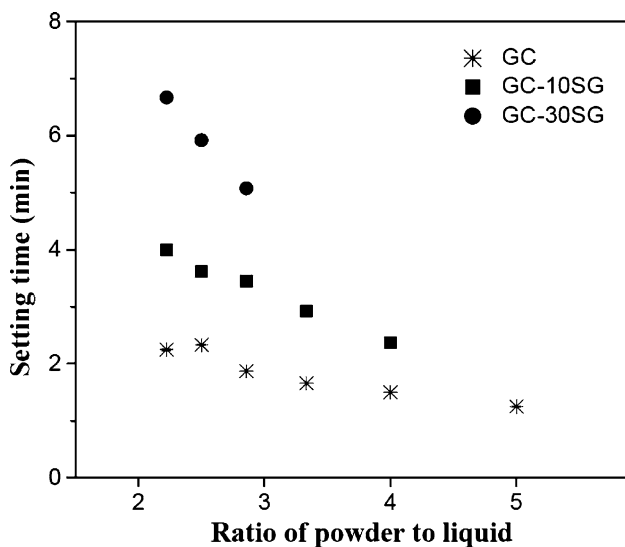


Fig. 3 Setting time of the dental cements without (GC) and with the addition of sol-gel derived bioactive glass powders (GC-10SG and GC-30SG)

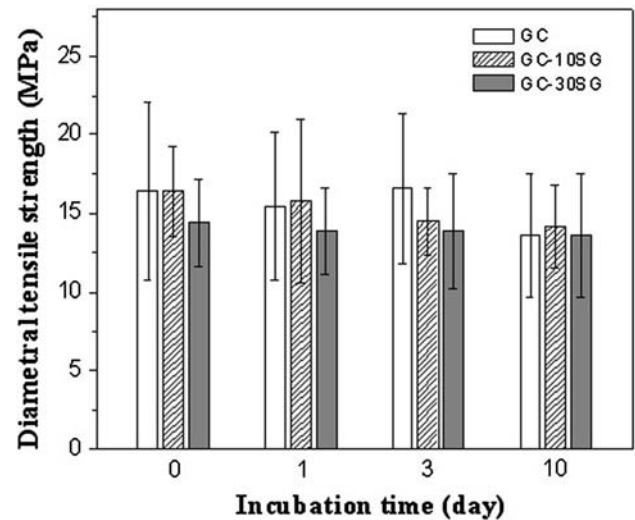


Fig. 4 Change in the diametral tensile strength of the dental cements before (0 day) and after the immersion in a simulated body fluid (1, 3 and 10 days). No significant difference was observed between the sample groups

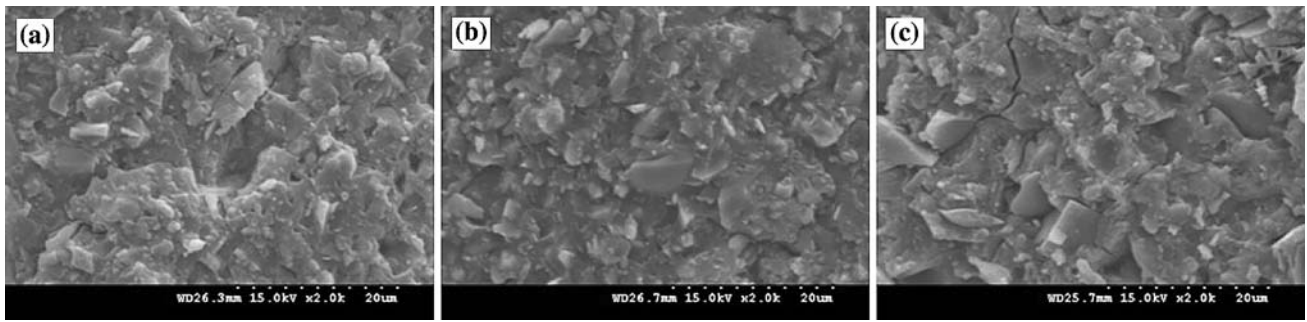
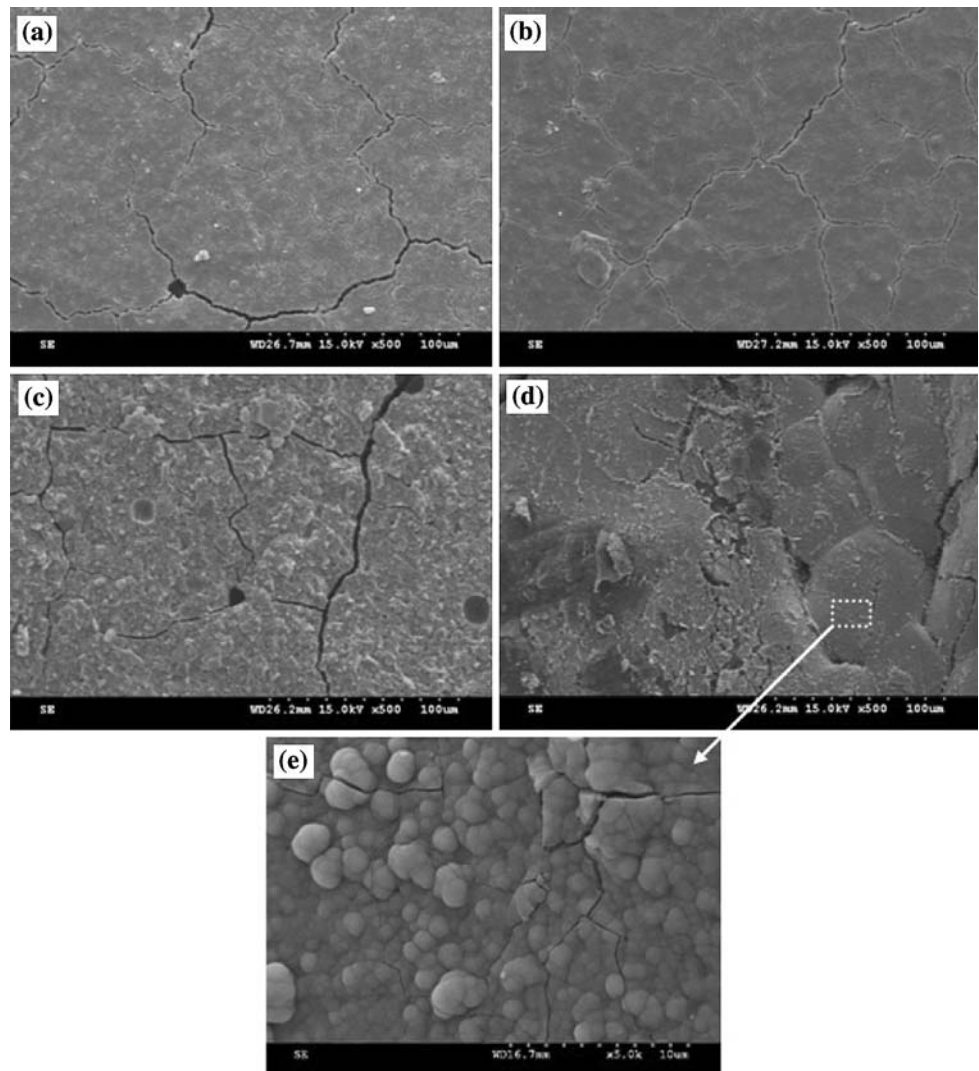


Fig. 5 SEM morphology of the fractured surface of the dental cements: (a) GC, (b) GC-10SG and (c) GC-30SG

Fig. 6 Surface morphological change of the dental cements (a, b) before and (c–e) after immersion in SBF for 14 days: (a, c) GC, (b, d, e) GC-30SG. Inset image in (d) is magnified in (e). On the surface of the GC-30SG cement, apatite bone-mineral phase was significantly induced



obtained is considered to be appropriate for dental cements in the regeneration field.

The DTS of the cements was measured, before and after immersion in SBF at 37°C for periods of up to 10 days. Figure 4 shows the DTS values of the three different types of cements with respect to the SBF-immersion period. The

as-prepared cements (0-day noted in the graph, which were pre-immersed in distilled water for 24 h) showed similar DTS values of ~16 MPa, even though GC-30SG showed a slightly lower value. During SBF-immersion, the DTS values of all the cement groups did not change significantly. The SEM fractured surface of the cement specimens

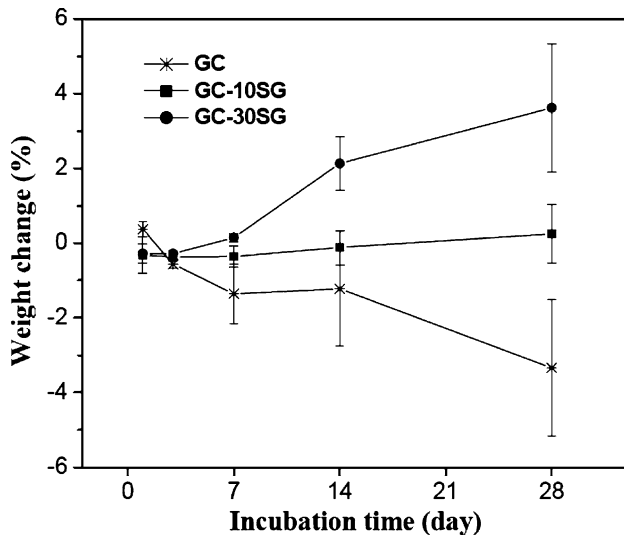


Fig. 7 Weight change in the dental cements after incubation in SBF for up to 28 days

observed after the strength test showed that all the cements were fractured in a similar manner with a rough fracture surface containing some pull-out of the large-sized powders, as shown in Fig. 5. Therefore, it was deduced that the addition of the sol-gel glass powder into the ionomer cement did not significantly degrade the tensile mechanical properties (particularly DTS) of the hardened cements and those after immersion in the SBF at least for up to 10 days.

3.3 Bioactivity and cell viability

The *in vitro* bioactivity of the prepared cements was assessed by immersing the cylindrical specimens in SBF and examining the level of apatite formation on the cement surface. Figure 6 shows the SEM image of the two different cements (GC and GC-30SG) before and after the immersion test for 14 days. Before immersion in the SBF, the surfaces of both cements were observed to be smooth but cracked to some extent (Fig. 6a, b). The cracking was deemed to be created by the pre-immersion in distilled

water and subsequent drying process. When GC was immersed in the SBF for 14 days, the surface appeared to become much rougher, which was attributed to the dissolution of materials (Fig. 6c). However, there was no indication of the mineral product induced on the GC surface. On the other hand, the surface of the GC-30SG cement showed dramatic changes after the SBF-immersion for 14 days (Fig. 6d). A higher magnification image clearly showed the formation of a bone-mineral apatite layer on the surface (Fig. 6e).

The weight change in the cement samples was monitored during the SBF-immersion test for up to 28 days, as shown in Fig. 7. In the GC sample, the initial weight decreased with immersion. However, no such decrease in weight was observed in the GC-SG cements. While the GC-10SG showed only a slight weight change, the GC-30SG exhibited a marked increase in weight during the immersion. Commercial ionomer cements including GC release ions such as sodium, silicon, aluminum, and

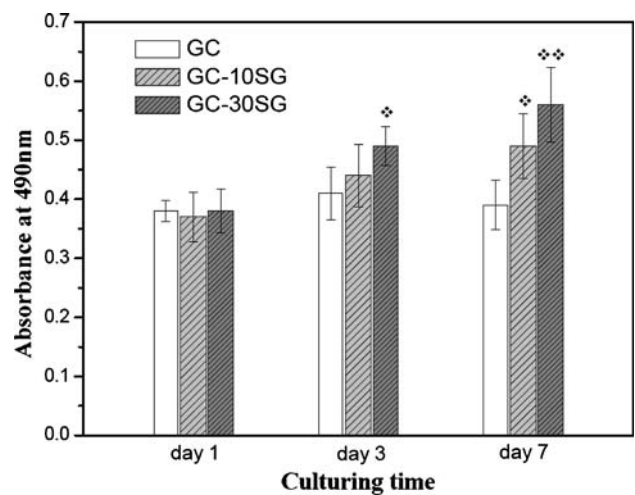
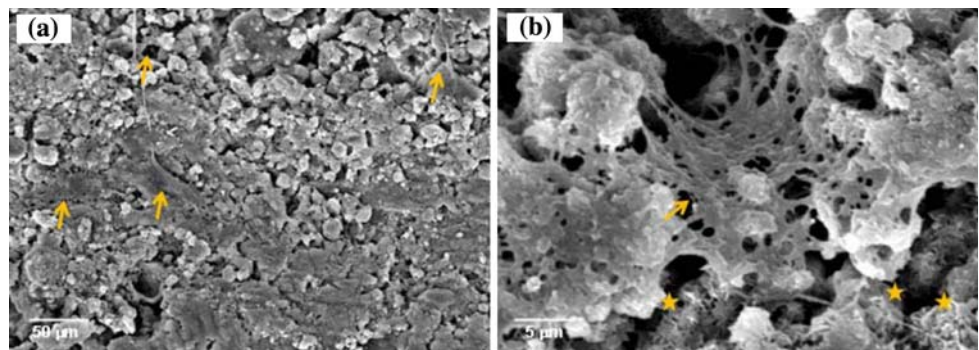


Fig. 9 Cell viability on the dental cements with culturing for up to 7 days, as assessed by the MTS method. A statistically significant difference was observed on the GC-SG group compared with the GC group ($n = 5$, ANOVA followed by Bonferroni, * $P < 0.05$ and ** $P < 0.01$)

Fig. 8 Electron micrographs of the MC3T3-E1 cells grown on the GC-30SG bioactive dental cements with 7 days of culturing. Cell image (arrowed in (a)) is magnified in (b) to show extensive cytoskeletal processes in intimate contact with underlying cement substrate. Apatitic crystals (star symbols) were shown to deposit during the cell culturing



fluoride within a fluid, resulting in a weight decrease [26]. In the GC–SG cements, calcium and phosphate ions in the sol–gel glass are also believed to be released from the cements. However, in this case, the released calcium and phosphate ions should readily precipitate on the cement surface, forming calcium phosphate mineral phase. Therefore, the different trend observed in the weight change of the GC–SG cements from that of the GC cement was attributed to both the dissolution of ions (weight loss) and their subsequent precipitation (weight gain). Based on the *in vitro* SBF-immersion test, the addition of a sol–gel bioactive glass into the ionomer cement is believed to improve the bone bioactivity of the dental cement by inducing the formation of an apatite mineral on the surface.

The cell viability on the prepared dental cements was assessed using osteoblastic cells (MC3T3-E1) with culturing for up to 7 days. Figure 8 shows the SEM morphologies of the cells grown on the GC–30SG cement for 7 days, as a representative example. The cells spread actively with extensive cytoskeletal processes in intimate contacts with the underlying cement surface. This was similarly observed in other cement groups. Of particular note was that apatitic crystallites (noted in star symbols in (b)) were induced on the surface of the bioactive cement.

Figure 9 shows the cell viability on the cements, as quantified by the MTS assay. The cells underwent considerable cell division on the cements with a continual increase over culturing periods of up to 7 days. Although similar at day 1, the level of cell growth was significantly higher on the bioactive glass-added cements (GC < GC–10SG < GC–30SG) at prolonged periods (particularly at day 7). This suggests that the addition of a sol–gel bioactive glass into the GC cement should alleviate the possible cytotoxic effect or stimulate the cellular division process. It is believed that the increased bioactivity of the GC–SG cements surface should favor the substrate-mediated cellular responses, namely the direct effect. Moreover, the ionic release from the bioactive glass is also expected to stimulate the cell growth level, *i.e.*, an indirect effect. In practice, the ions released from the bioactive glasses including the sol–gel glass were reported to play significant roles in stimulating cell growth and osteoblastic differentiation [27, 28].

Overall, the added bioactive glass might affect the osteoblastic cell growth either directly through the bioactive substrate and/or indirectly by the role of the releases ions. Although further studies of the cellular processes on the cements, such as cell differentiation and mineralization, are still required, this study delivers at least the beneficial role of the bioactive sol–gel glass within the GC cement composition in the initial cell growth stage. The enhanced bone bioactivity of the sol–gel glass added GC cement in

the SBF condition also supports its usefulness in the regeneration of tooth structure.

4 Conclusions

Sol–gel derived bioactive glass powder was added at 10 and 30 wt% to the dental ionomer cement (GC, Fuji I). The setting of the bioactive glass added cements was retarded by up to a few minutes compared with the pure ionomer cement. The addition of a bioactive glass did not show any significant decrease in DTS with respect to the pure ionomer cement. Moreover, the cements maintained the initial DTS values after immersion in SBF for up to 10 days. During SBF-immersion, the bioactive glass added cements induced the formation of apatite minerals on the surface, which was not observed in the case of the pure ionomer cement. Tissue cells adhered and spread more favorably on the glass-added cements, with a higher level of cell growth than that of the pure ionomer cement. Based on this study, the bioactive glass added ionomer cements might be useful for regenerating the tooth structure.

Acknowledgement The present research was conducted by the research fund of Dankook University in 2006.

References

1. A.D. Wilson, B.E. Kent, *Br. Dent. J.* **132**, 133–135 (1972)
2. S.K. Sidhu, T.F. Watson, *Am. J. Dent.* **8**, 59–67 (1995)
3. A.W.G. Walls, *J. Dent.* **14**, 231–246 (1986)
4. D. Xie, B.M. Brantley, G. Culbertson, G. Wang, *Dent. Mater.* **16**, 129–138 (2000)
5. S.R. Grobler, R.J. Rossouw, T.J. Van Wyk Kotze, *J. Dent.* **26**, 259–265 (1998)
6. A.D. Wilson, D.M. Groffman, A.T. Kuhn, *Biomaterials* **6**, 431–433 (1985)
7. L. Forsten, *Biomaterials* **19**, 503–508 (1998)
8. C.A.S. Costa, J. Hebling, F. Garcia-Godoy, C.T. Hanks, *Biomaterials* **24**, 3826–3858 (2003)
9. F.M. Huang, Y.C. Chang, *Oral Surg. Oral Med. Oral Pathol. Oral Radiol. Endod.* **94**, 361–365 (2002)
10. I.M. Brook, P.V. Hatton, *Biomaterials* **18**, 565–571 (1998)
11. D.H. Carter, P. Sloan, I.M. Brook, P.V. Hatton, *Biomaterials* **18**, 459–466 (1997)
12. D. Boyd, M.R. Towler, *J. Mater. Sci.: Mater. Med.* **16**, 843–850 (2005)
13. R.T. Ramsden, R.C.D. Herdman, R.H. Lye, *J. Laryngol. Otol.* **106**, 949–953 (1992)
14. J.T. McElveen, *Otolaryngol. Clin. North Am.* **27**, 777–784 (1994)
15. M.A. Cattani-Lorente, C. Godin, J.M. Meyer, *Dent. Mater.* **9**, 57–62 (1993)
16. M.A. Cattani-Lorente, C. Godin, J.M. Meyer, *Dent. Mater.* **10**, 37–44 (1994)
17. S.B. Mitra, B.L. Dedrowski, *Dent. Mater.* **10**, 78–82 (1994)
18. A.J. de Gee, R.N. van Duinen, A. Werner, C.L. Davidson, *J. Dent. Res.* **75**, 1613–1619 (1996)

19. P.H. Hantson, P. Mahieu, M. Gersdorff, C.J.M. Sindic, R. Lauwerys, *Lancet* **344**, 1647 (1994)
20. A.U.J. Yap, Y.S. Pek, R.A. Kumar, P. Cheang, K.A. Khor, *Biomaterials* **23**, 955–962 (2002)
21. H. Yli-Urpo, M. Narhi, T. Narhi, *Biomaterials* **26**, 5934–5941 (2005)
22. Y.W. Gu, A.U.J. Yap, P. Cheang, K.A. Khor, *Biomaterials* **26**, 713–720 (2005)
23. R.E. Kerby, R.F. Bleiholder, *J. Dent. Res.* **70**, 1358–1361 (1991)
24. J.P. Zhong, D.C. Greenspan, *J. Biomed. Mater. Res.* **53**, 694–701 (2000)
25. A.J. Salinas, A.I. Martin, M. Vallet-Regi, *J. Biomed. Mater. Res.* **61**, 524–532 (2002)
26. J.W. Nicholson, *Biomaterials* **19**, 485–494 (1998)
27. I.D. Xynos, A.J. Edgar, D.K. Lee, L.D. Buttery, L.L. Hench, J.M. Polak, *J. Biomed. Mater. Res.* **55**, 151–157 (2001)
28. S. Hattar, S. Loty, D. Gaisser, A. Berdal, J.M. Sautier, *J. Biomed. Mater. Res. A* **76A**, 811–819 (2006)